Supplementary Information for

Characterization of AusA: A Dimodular Nonribosomal Peptide Synthetase Responsible for Production of Aureusimine Pyrazinones

*Daniel J. Wilson,[1] Ce Shi,[1] Aaron M. Teitelbaum,[2] Andrew M. Gulick,[3] Courtney C. Aldrich[1]**

[1]Center for Drug Design, University of Minnesota, Minneapolis, Minnesota 55455; [2]Department of Medicinal Chemistry, University of Minnesota, Minneapolis, Minnesota, MN 55455; [3]Hauptman-Woodward Institute and Department of Structural Biology, University at Buffalo, Buffalo, NY, 14203 USA.

Table of Contents

Scheme S1.[a] Synthesis of **1-4**

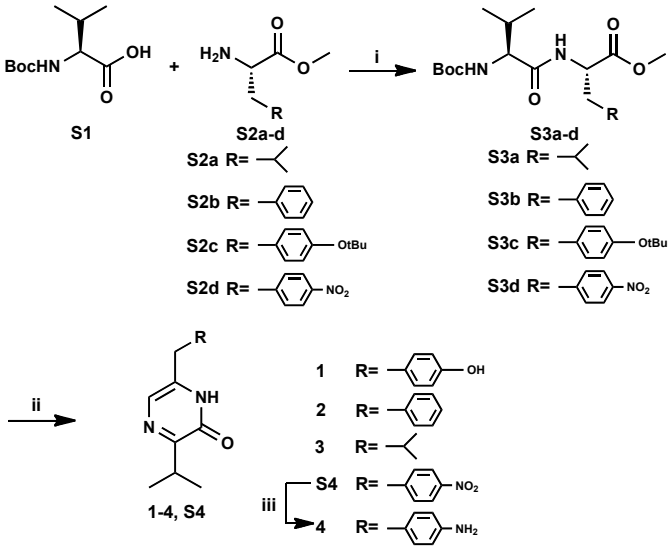

[a]Conditions: i) HBTU, EtN(iPr)$_2$, THF-CH_3CN, 78-93%; ii) a) DIBAL-H, CH_2Cl_2, -78 ^oC; b) CF_3CO_2H, anisole, CH_2Cl_2; c) NEt_3, 2-Butanol-Toluene, 100 ^oC, 45-56% over 3 steps. iii) Pd/C, H_2, MeOH, 95%.

Scheme S2.[a] Synthesis of Val-AMS (**5**)

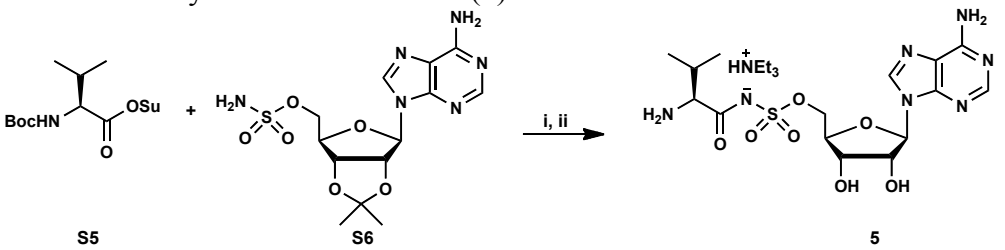

[a]Conditions: i) Cs_2CO_3, DMF, 0 ^oC–25 ^oC, 15 h; ii) TFA:H_2O (8:2), 0 ^oC–25 ^oC, 1 h, 56% over 2 steps.

Scheme S3.[a] Synthesis of tyrosinol **S8** and tyrosinal oxime **S10.**

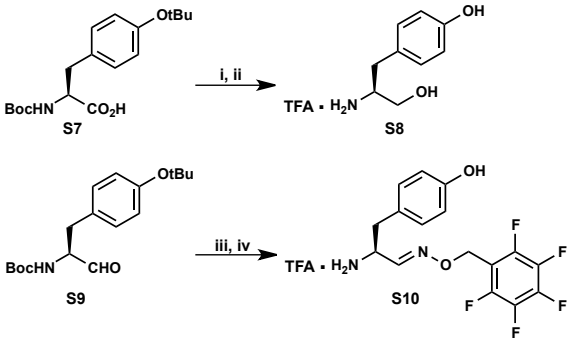

[a]Conditions: i) $LiAlH_4$, THF, 0 ^oC, 83%; ii) TFA, CH_2Cl_2, 67%; iii) *O*-(2,3,4,5,6-penta-fluorobenzyl)hydroxylamine·HCl (PFBHA·HCl), NEt_3, MeOH, reflux, 76%; iv) TFA, CH_2Cl_2, 75%.

Chemical synthesis

General methods: All chemical reactions were performed under an inert atmosphere of dry Ar or N_2 in oven-dried (150 °C) glassware. ^{1}H and ^{13}C NMR spectra were recorded on a Varian 600 MHz or a Varian 400 MHz spectrometer. Proton chemical shifts are reported in ppm from an internal standard of residual chloroform (7.26 ppm) or methanol (3.31 ppm) and carbon chemical shifts are reported using an internal standard of residual chloroform (77.0 ppm) or methanol (49.1 ppm). Proton chemical data are reported as follows: chemical shift, multiplicity (s = singlet, d = doublet, t = triplet, q = quartet, p = pentet, hex = sextet, hept = septet, m = multiplet, br = broad), coupling constant, integration. High resolution mass spectra were obtained on an Agilent TOF II TOF/MS instrument equipped with either an ESI or APCI interface. TLC analyses were performed on TLC silica gel 60F254 from EMD Chemical Inc., and were visualized with UV light, iodine chamber, 10% sulfuric acid or 10% PMA solution. Optical rotations values were obtained on a Rudoldf Autopol III Polarimeter. Purifications were performed by flash chromatography on silica gel (Dynamic Adsorbents, 60A).

Materials: Chemicals and solvents were purchased from Sigma-Aldrich Company, Acros Organic Fischer Company, TCI America Company or Chem-Impex International Inc., and were used as received. An anhydrous solvent dispensing system (J. C. Meyer) using 2 packed columns of neutral alumina was used for drying THF, Et_2O, and CH_2Cl_2 while 2 packed columns of molecular sieves were used to dry DMF and the solvents were dispensed under argon. 5'-*O*-[*N*-[L-Phenylalanyl]sulfamoyl]adenosine sodium salt was synthesized according to the reported procedures.[1] Boc-(O*t*Bu)Tyr-H was purchased from Chem-Impex, and *O*-(2,3,4,5,6-pentafluorobenzyl)hydroxylamine·HCl (PFBHA·HCl) was purchased from Sigma-Aldrich. Boc-(O*t*Bu)Tyr-CHO was synthesized according to the reported procedure.[13]

Boc-Val-Leu-OMe (**S3a**) To a suspension of Boc-Val-OH (434 mg, 2.0 mmol, 1.0 equiv) and HCl·H-Leu-OMe (362 mg, 2.0 mmol, 1.0 equiv) in THF (10 mL) and CH_3CN (4 mL) at 25 °C, was added HBTU (833 mg, 2.2 mmol, 1.1 equiv) and $EtN(iPr)_2$ (1.0 mL, 6.0 mmol, 3.0 equiv) sequentially. The reaction was stirred for 2 h and concentrated in vacuo. The mixture was then partitioned between EtOAc (50 mL) and cold 5% citric acid (20 mL). The organic layer was washed by water (20 mL), saturated $NaHCO_3$ aqueous solution (20 mL) and saturated NaCl aqueous solution (20 mL), dried ($MgSO_4$) and concentrated. Purification by flash column chromatography on silica gel (1:9 EtOAc/Hexanes–3:7 EtOAc/Hexanes) afforded the title compound as colorless foam (612 mg, 89%): R_f 0.65 (1:1, EtOAc/Hexanes); ^{1}H NMR ($CDCl_3$, 600 MHz) δ 0.92–0.93 (m, 9H), 0.96 (d, J = 7.2 Hz, 3H), 1.44 (s, 9H), 1.53–1.57 (m, 1H), 1.61–1.67 (m, 2H), 2.11 (br s, 1H), 3.72 (s, 3H), 3.88 (t, J = 6.6 Hz, 1H), 4.61 (dt, J = 9.0, 4.8 Hz, 1H), 5.02 (br s, 1H), 6.19 (br s, 1H); ^{13}C NMR ($CDCl_3$, 150 MHz) δ 17.9, 19.2, 21.8, 22.8, 24.7, 28.3, 30.8, 41.6, 50.6, 52.2, 60.0, 79.9, 155.8, 171.4, 173.1; HRMS (APCI+): calcd $C_{17}H_{32}N_2O_5$ $[M + H]^+$ 345.2389, found 345.2392 (error 0.9 ppm). All data are consistent with reported values.[2]

Boc-Val-Phe-OMe (**S3b**) The title compound was prepared analogously to **S3a** and obtain as colorless foam in 93% yield: R_f 0.7 (1:1, EtOAc/Hexanes); ^{1}H NMR ($CDCl_3$, 600 MHz) δ 0.87 (d, J = 6.0 Hz, 3H), 0.91 (d, J = 6.0 Hz, 3H), 1.44 (s, 9H), 2.07 (br s, 1H), 3.07–3.15 (m, 2H), 3.89 (d, J = 6.6 Hz, 1H), 4.84–4.88 (m, 1H), 5.00 (br s, 1H), 6.29 (br s, 1H), 7.10 (d, J = 7.2 Hz, 2H), 7.21–7.29 (m, 3H); ^{13}C NMR ($CDCl_3$, 150 MHz) δ 17.6, 19.1, 28.3, 30.8, 38.0, 52.3, 53.1,

59.9, 79.9, 127.2, 128.6, 129.2, 135.6, 155.7, 171.2, 171.6; All data are consistent with reported values.[3]

Boc-Val-Tyr(OtBu)-OMe (**S3c**) The title compound was prepared analogously to **S3a** and obtain as colorless foam in 90% yield: R_f 0.55 (1:1, EtOAc/Hexanes); $[\alpha]_D^{23}$ = +28 (*c* 0.6, CH_2Cl_2); ^{1}H NMR ($CDCl_3$, 600 MHz) δ 0.85 (br d, *J* = 6.0 Hz, 3H), 0.91 (d, *J* = 6.0 Hz, 3H), 1.32 (s, 9H), 1.44 (s, 9H), 2.06–2.10 (m, 1H), 3.06 (d, *J* = 4.8 Hz, 2H), 3.67 (s, 3H), 3.90 (br s, 1H), 4.82 (q, *J* = 6.0 Hz, 1H), 4.99 (br s, 1H), 6.29 (br s, 1H), 6.89 (d, *J* = 8.4 Hz, 2H), 7.00 (d, *J* = 8.4 Hz, 2H); ^{13}C NMR ($CDCl_3$, 150 MHz) δ 17.6, 19.1, 28.3, 28.8, 30.8, 37.4, 52.2, 53.1, 59.8, 78.4, 79.8, 124.2, 129.6, 130.4, 154.5, 171.1, 171.7; HRMS (APCI+): calcd $C_{24}H_{39}N_2O_5$ $[M + H]^+$ 451.2808, found 451.2807 (error 0.3 ppm).

Boc-Val-Phe(*p*-NO_2)-OMe (**S3d**) The title compound was prepared analogously to **S3a** and obtain as colorless foam in 93% yield: R_f 0.35 (1:1, EtOAc/Hexanes); ^{1}H NMR ($CDCl_3$, 600 MHz) δ 0.89 (br d, *J* =7.2 Hz, 3H), 0.93 (d, *J* =7.2 Hz, 3H), 1.43 (s, 9H), 2.07 (br s, 1H), 3.16 (dd, *J* = 13.2, 6.0 Hz, 1H), 3.30 (dd, *J* = 13.2, 6.0 Hz, 1H),3.74 (s, 3H), 3.84 (t, J = 6.0 Hz, 1H), 4.91 (t, *J* = 6.0 Hz, 1H), 7.32 (d, *J* = 9.0 Hz, 2H), 8.15 (d, *J* = 9.0 Hz, 2H); ^{13}C NMR ($CDCl_3$, 150 MHz) δ 17.9, 19.2, 28.3, 30.5, 37.9, 52.6, 52.7, 60.2, 80.1, 123.7, 130.2, 143.6, 147.2, 171.0, 171.4; HRMS (APCI+): calcd $C_{20}H_{30}N_3O_7$ $[M + H]^+$ 424.2084, found 424.2084 (error 0.0 ppm). All data are consistent with reported values.[4]

6-Isobutyl-3-isopropylpyrazin-2(1*H*)-one (**3**) To a solution of **S3a** (196 mg, 0.57 mmol, 1.0 equiv) in CH_2Cl_2 (5 mL) at -78 ^{o}C, was added 1M DIBAL-H in CH_2Cl_2 solution (4.0 mL, 4.0 mmol, 4.0 equiv) dropwise over 10 min. The solution was stirred for 1 h and quenched by MeOH (0.5 mL) and 1N potassium sodium tartrate aqueous solution (20 mL). The mixture was gradually warmed up to 25 ^{o}C and stirred for 30 min. The aqueous layer was extracted with CH_2Cl_2 (3 × 20 mL) and the combined organic layer was washed with water (20 mL), saturated NaCl aqueous solution, dried ($MgSO_4$) and concentrated in vacuo to afford the crude aldehyde intermediate which was used in the next step without further purification.

The crude aldehyde was dissolved in CH_2Cl_2 (1 mL) containing CH_3CO_2H (1 mL) and anisole (80 μL). The reaction was stirred at 25 ^{o}C for 30 min and concentrated in vacuo to afford the crude amino-aldehyde intermediate, which was used in the next step without further purification.

The crude amino-aldehyde intermediate was dissolved in 2-butanol (4 mL) and toluene (1 mL). To this solution was added NEt_3 (80 uL, 0.6 mmol, 1.1 equiv). The reaction was heated to 100 ^{o}C and stirred for 15 h before cooled to 25 ^{o}C and concentrated in vacuo. Purification by flash column chromatography on silica gel (CH_2Cl_2–1:9, MeOH/CH_2Cl_2) afforded the title compound as off white solid (89 mg, 46%): R_f 0.65 (1:9, MeOH/CH_2Cl_2); ^{1}H NMR ($CDCl_3$, 600 MHz) δ 0.97 (d, *J* = 6.6 Hz, 6H), 1.24 (d, *J* = 7.2 Hz, 6H), 2.04 (hept, *J* = 6.6 Hz, 1H), 2.38 (d, *J* = 6.6 Hz, 2H), 3.40 (hept, *J* = 6.6 Hz, 1H), 7.19 (s, 1H); ^{13}C NMR ($CDCl_3$, 150 MHz) δ 19.9, 22.2, 28.2, 30.2, 39.5, 123.0, 127.3, 157.7, 161.2; HRMS (APCI+): calcd $C_{11}H_{19}N_2O$ $[M + H]^+$ 195.1497, found 195.1498 (error 0.5 ppm). All data are consistent with reported values.[5]

6-Benzyl-3-isopropylpyrazin-2(1*H*)-one (**2**) The title compound was prepared analogously to **3** and obtain as colorless foam in 63% yield: mp 117.5–118.5 ^{o}C; R_f 0.55 (1:9, MeOH/CH_2Cl_2); ^{1}H NMR (CD_3OD, 600 MHz) δ 1.17 (d, *J* = 6.6 Hz, 6H), 3.35 (hept, *J* = 6.6 Hz,

1H), 3.76 (s, 2H), 7.17–7.20 (m, 3H), 7.22–7.27 (m, 3H); ^{13}C NMR (CD_3OD, 150 MHz) δ 20.0, 30.1, 36.6, 122.2, 127.4, 128.9, 129.1, 135.9, 136.8, 157.4, 162.0; All data are consistent with the reported value.[6]

6-(4-Hydroxybenzyl)-3-isopropylpyrazin-2(1*H*)-one (**1**) The title compound was prepared analogously to **3** and obtain as colorless foam in 55% yield: R_f 0.55 (1:9, MeOH/CH_2Cl_2); ^{1}H NMR (CD_3OD, 600 MHz) δ 1.18 (d, J = 7.2 Hz, 6H), 3.34 (hept, J = 6.0 Hz, 1H), 3.73 (s, 2H), 6.74 (d, J = 9.0 Hz, 2H), 7.07 (d, J = 9.0 Hz, 2H), 7.08 (s, 1H); ^{13}C NMR (CD_3OD, 150 MHz) δ 20.6, 31.1, 36.3, 116.7, 123.3, 128.6, 131.1, 140.2, 145.4, 156.8, 158.1; HRMS (APCI+): calcd $C_{14}H_{17}N_2O_2$ $[M + H]^+$ 245.1290, found 245.1294 (error 1.6 ppm). All data are consistent with the reported value.[7]

3-Isopropyl-6-(4-nitrobenzyl)-pyrazin-2(1*H*)-one (**S4**) The title compound was prepared analogously to **3** and obtain as yellow solid in 43% yield: R_f 0.55 (1:9, MeOH/CH_2Cl_2); ^{1}H NMR ($CDCl_3$, 600 MHz) δ 1.24 (d, J = 7.2 Hz, 6H), 3.38 (hept, J = 7.2 Hz, 1H), 3.93 (s, 2H), 7.31 (s, 1H), 7.54 (d, J = 9.0 Hz, 2H), 8.17 (d, J = 9.0 Hz, 2H); ^{13}C NMR (CD_3OD, 150 MHz) δ 19.9, 30.2, 36.4, 122.9, 124.0, 130.1, 135.0, 143.5, 147.3, 157.6, 162.7; HRMS (APCI+): calcd $C_{14}H_{16}N_3O_3[M + H]^+$ 274.1192, found 274.1199 (error 2.6 ppm).

6-(4-Aminobenzyl)-3-isopropylpyrazin-2(1*H*)-one (**4**) To a solution of **S4** (136 mg, 0.5 mmol, 1.0 equiv) in MeOH (5 mL), was added Pd/C 10 wt% (53 mg, 0.05 mmol, 10 mol%). The reaction was kept under H_2 atmosphere (30 psi) for 3 h with vigorous stirring. The suspension was filtered over a pad of Celite and washed with MeOH (3 × 15 mL). The filtrate was concentrated in vacuo to afford the crude. Purification by flash column chromatography on silica gel (CH_2Cl_2–1:9, MeOH/CH_2Cl_2) afforded the title compound as off white solid (115 mg, 95%): R_f 0.45 (1:9, MeOH/CH_2Cl_2); ^{1}H NMR (CD_3OD, 400 MHz) δ 1.18 (d, J = 6.8 Hz, 6H), 3.34 (hept, J = 6.8 Hz, 1H), 3.69 (s, 2H), 6.68 (d, J = 8.0 Hz, 2H), 7.00 (d, J = 8.0 Hz, 2H), 7.07 (s, 1H); ^{13}C NMR (CD_3OD, 150 MHz) δ 20.5, 31.1, 36.4, 117.0, 123.2, 127.1, 130.7, 140.3, 148.0, 158.0, 162.5; HRMS (ESI+): calcd $C_{14}H_{16}N_3O_3[M + H]^+$ 244.1450, found 244.1455 (error 2.0 ppm).

5'-*O*-[*N*-[L-Valinyl]sulfamoyl]adenosine triethylammonium salt (**5**) To a solution of sulfamoyladenosine **S6 (**38.7 mg, 0.1 mmol, 1.0 equiv) and Boc-Val-OSu **S5** (60 mg, 0.2 mmol, 2.0 equiv) in DMF (1 mL) at 0 °C, was added Cs_2CO_3 (97 mg, 0.3 mmol, 3.0 equiv) in one portion. The mixture was gradually warmed up to 25 °C and stirred for 15 h. The reaction was concentrated in vacuo and redissolved in MeOH/CH_2Cl_2 (1/9, 20 mL). Filtration over celite and concentration in vacuo afforded the crude 2',3'-isopropylidene-5'-*O*-[*N*-(*N*-Boc-*L*-valinyl)sulfamoyl]adenosine which was used directly in the next step without further purification.

The crude 2',3'-isopropylidene-5'-*O*-[*N*-(*N*-Boc-*L*-valinyl)sulfamoyl]adenosine was dissolved in TFA/H_2O (8/2, 2 mL) at 0 °C, gradually warmed up to 25 °C, and was stirred for 1 h. The reaction was quenched by addition of NEt_3 (0.5 mL) and concentrated in vacuo. The crude was dissolved in MeOH/H_2O (1/1, 1.5 mL) and purified by preparative HPLC (injected 3 × 500 µL) using a Varian Dynamax Microsorb 100-8 C18 column (250 × 41.4 mm) and a linear gradient of 5–40% MeOH/10 mM triethylammonium bicarbonate (pH 7.0) over 10 min followed by 40% MeOH for 10 min at 35 mL/min. The retention time of the product was 16.3 min and the

appropriate fractions were pooled and lyophilized to afford the title compound (30 mg, 56% in 2 steps) as a white solid. ^{1}H NMR (CD_3OD, 600 MHz) δ 0.95 (d, J = 6.6 Hz, 3H), 1.02 (d, J = 6.6 Hz, 3H), 1.13 (t, J = 7.2 Hz, 9H), 2.17 (br s, 1H), 2.78 (q, J = 7.2 Hz, 6H), 4.28–4.31 (m, 3H), 4.35–4.37 (m, 1H), 4.40 (t, J = 4.2 Hz, 1H), 4.64 (t, J = 5.4 Hz, 1H), 6.08 (d, J = 5.4 Hz, 1H), 8.20 (s, 1H), 8.52 (s, 1H); ^{13}C NMR (CD_3OD, 150 MHz) δ 10.6, 17.7, 17.8, 20.0, 47.4, 69.2, 72.2, 76.3, 84.5, 86.3, 89.5, 120.3, 141.4, 150.9, 154.0, 157.4, 176.4; HRMS (ESI–): calcd $C_{15}H_{22}N_7O_7S$ $[M - H]^-$ 444.1301, found 444.1304 (error 0.7 ppm). All data are consistent with the reported value.[8]

(*L*)-Tyrocinol (S8). To a solution of Boc-(O*t*Bu)Tyr-H **S7** (337 mg, 1.0 mmol, 1.0 equiv) in THF (10 mL) at 0 °C, was added $LiAlH_4$ (114 mg, 3.0 mmol, 3.0 equiv) portion-wise over 10 min. The mixture was stirred for 1 h at 0 °C and quenched by addition of MeOH (0.5 mL) and Rochelle salt solution (20 mL). The layers were separated after stirring at 25 °C for 30 min. The aqueous layer was extracted with EtOAc (20 × 3 mL). The combined organic layer was extracted with H_2O (20 mL), washed with saturated NaCl aqueous solution (20 mL), dried ($MgSO_4$) and concentrated to afford the crude product. Purification by flash column chromatography on silica gel (1:9 EtOAc/Hexanes–5:5 EtOAc/Hexanes) afforded the *N*-Boc-tyrocinol as colorless oil (268 mg, 83%): R_f 0.55 (5:5, EtOAc/Hexanes); ^{1}H NMR ($CDCl_3$, 600 MHz) δ 1.30 (s, 9H), 1.38 (s, 9H), 2.75 (br s, 2H), 3.48–3.49 (m, 1H), 3.57–3.60 (m, 1H), 3.81 (br s, 1H), 4.91 (br s, 1H), 6.88 (d, J = 7.8 Hz, 2H), 7.07 (d, J = 7.8 Hz, 2H); All data are consistent with reported values.[14]

To a solution of *N*-Boc-tyrocinol (64 mg, 0.2 mmol, 1.0 equiv) in CH_2Cl_2 (4 mL) at 0 °C, was add CF_3CO_2H (2 mL). The solution was stirred for 1 h and concentrated in vacuo. Pure tyrocinol TFA salt (44 mg, 83%) was obtained after precipitation from Et_2O/MeOH (20:1). ^{1}H NMR (CD_3OD, 600 MHz) δ 2.45 (dd, J = 13.8, 7.8 Hz, 1H), 2.68 (dd, J = 13.8, 6.0 Hz, 1H), 2.89–2.91 (m, 1H), 3.33–3.35 (m, 1H), 3.54–3.56 (m, 1H), 6.72 (d, J = 7.8 Hz, 2H), 7.02 (d, J = 7.8 Hz, 2H); LRMS (APCI+): 168.3. All data are consistent with reported values.[15]

(*L*)-Tyrocinal-*O*-perfluorobenzyl oxime (S10).To a solution of *N*-Boc-tyrocinal[13] (64 mg, 0.2 mmol, 1.0 equiv) and PFBHA·HCl (53 mg, 0.21 mmol, 1.05 equiv) in MeOH (5 mL) at 25 °C, was added NEt_3 (30 µL, 0.22 mmol, 1.1 equiv). The solution was heated up to reflux for 6 h. The reaction was concentrated in vacuo and reconstituted in CH_2Cl_2 (50 mL). The solution was washed 1N HCl aqueous solution (20 mL), H_2O (20 mL) and saturated NaCl aqueous solution (20 mL), dried ($MgSO_4$) and concentrated to afford the crude. Purification by flash column chromatography on silica gel (Hexanes–1:9 EtOAc/Hexanes) afforded the *N*-Boc-tyrocinal-*O*-perfluorobenzyl oxime as off white solid (79 mg, 76%): R_f 0.65 (2:8, EtOAc/Hexanes); ^{1}H NMR ($CDCl_3$, 600 MHz) δ 1.32 (s, 9H), 1.41 (s, 9H), 2.85–2.93 (m, 2H), 4.49 (br s, 1H), 4.89 (br s, 1H), 5.09 (s, 2H), 6.88 (d, J = 7.8 Hz, 2H), 7.02 (d, J = 7.8 Hz, 2H), 7.34 (br s, 1H). LRMS (APCI+): 517.4.

To a solution of *N*-Boc-tyrocinal-*O*-perfluorobenzyl oxime (62 mg, 0.12 mmol, 1.0 equiv) in CH_2Cl_2 (4 mL) at 0 °C, was add CF_3CO_2H (2 mL). The solution was stirred for 1 h and concentrated in vacuo. Pure (*L*)-Tyrocinal-*O*-perfluorobenzyl oxime TFA salt (41 mg, 75%) was obtained after precipitation from Et_2O/MeOH (20:1); ^{1}H NMR (CD_3OD, 600 MHz) δ 2.92–3.00 (m, 2 H), 4.10–4.14 (m, 1H), 5.17–5.18 (m, 2H), 6.72 (d, J = 7.8 Hz, 2H), 7.00 (d, J = 7.8 Hz, 2H), 7.00 (d, J = 4.2 Hz, 1H). LRMS (ESI+): 361.2.

The first NRPS adenylation domain to be crystallized was the phenylalanine activiting domain of the gramicidin synthetase protein, GrsA.[9] This structure served as the basis for an analysis of the residues that contribute to the amino acid substrate binding pocket allowing predictions to be made for uncharacterized NRPS proteins.[10] We examined the predicted binding pocket for the valine-activating adenylation domain of AusA in the context of this analysis and, in particular, in light of the recent crystal structure determination of PA1221, a valine-specific adenylating protein that was crystallized in the presence of the valine-adenosine vinylsulfonamide inhibitor that illustrates how valine binds in the binding pocket.[11] Examination of the valine binding pocket of PA1221, as well as a three-dimensional homology model generated by the PHYRE server[12] illustrates that the residues of the PA1221 valine binding pocket, Asp214, Ala215, Trp256, Thr214, and Phe315 all are retained in the AusA sequence at positions 609, 610, 652, 710, and 711, respectively (Figure S1). Indeed, among the ten residues identified by Stachelhaus, the only difference between the AusA and PA1221 sequences is a change from Leu218 in PA1221 to Phe612 in AusA. The large side chains of Trp256 and Phe315 seal off the valine binding pocket, leaving Leu218–or Phe612 in AusA–contributing to the hydrophobic core of the protein.

A)

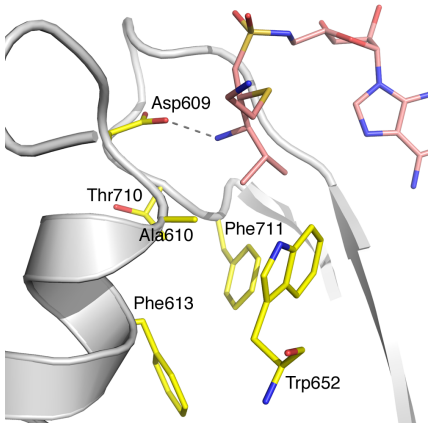

B)

```
GrsA          166    --TIKIREGTNLHVPSKSTDLAYVIYTSGTTGNPKGTMLEHKGISNLKVFFENSLNVTEKDRIGQFASISFDAS
AusA Aden1    541    --KIAWKNIDNLSKCNTLEDHAYVIYTSGTTGNPKGTLIPHRGIVRLVHQNH-YVPLNEKTTILLSGTIAFDAA
PA1221        146    --HLPAAPASVARPCFAADQIAYINFSSGTTGRPKAIACTHAGITRLCLGQS-FLAFAPQMRFLVNSPLSFDAA
                                        **    ***** **     * **  *                    ***

GrsA          238    VWEMFMALLTGASLYIILKDTINDFVKFEQYINQKEITVITLPPTYVVHLDPE---RILSIQTLITAGSATSPS
AusA Aden1    612    TFEIYGALLNGGKLIVAKKEQLLNPIVLEQLINENDVNTMWLTSSLFNQIASERIEVLVPLKYLLIGGEVLNAK
PA1221        217    TLEIWGALLNGG-CCVLNDLGPLDPGVLRQLIGERGADSAWLTASLFNTLVDLDPDCLGGLRQLLTGGDILSVP
                       *   *** *                 * *         *.                  *  *  *

GrsA          309    LVNKWKEKVT---YINAYGPTETTICATTWVATKETIGHS-VPIGAPIQNTQIYIVDEN-LQLKSVGEAGELCI
AusA_Aden1    686    WVDLLNQRPKHPQIINGYGPTENTTFTTTYNIPNKVPNR--IPIGKPILGTHVYIMQGE-RRCG-VGIPGELCT
PA1221        290    HVRRALLRHPRLHLVNGYGPTENTTFTCCHVVTDDDLEEDDIPIGKAIAGTAVLLLDEHGQEIAEPDRAGEIVA
                      *           * ***** *                  ***  *  *                    **
```

Figure S1. A) Protein homology model for the valine binding pocket of the AusA adenylation domain of the first module. The residues that form the valine pocket are highlighted in yellow. Superimposed in pink is ligand from the PA1221 crystal structure showing the valine-adenosine vinylsulfonamide that has reacted with the pantetheine group from the carrier protein domain. **B)** A partial sequence alignment is shown for GrsA, AusA, and PA1221. The residues identified by Stachelhaus as forming the amino acyl binding pocket of NRPS adenylation domains are highlighted in yellow. Residues conserved among all three proteins are highlighted in blue. The Leu218 and Phe612 change is shown in red.

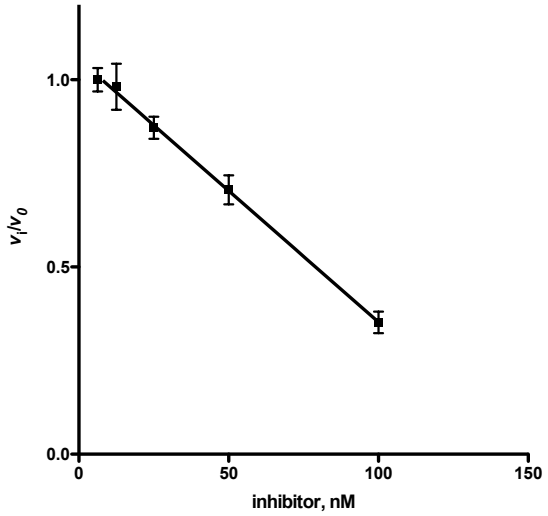

Figure S2. AusA titration. Each reaction contained 200 nM holo AusA, 3.1 — 400 nM Phe-AMS, 375 mM Bicine pH 8.0, 10 mM $MgCl_2$, 0.2 mM ATP, 0.1 mM NADPH, 1 mM TCEP, 3 mM L-Val and 0.2 mM L-Tyr. Fractional velocities were fit using linear regression and the x-intercept provides the active enzyme concentration.

A)

```
PstD/569–885      TVLLTGATGFLGRYLVLELLRRL
PznA/2055–2290    KTLLTGATGFLGAYLIEALQGYS
KorD/616–895      NIMITGGTGFLGAHLLNKLLMEM
LgrD/4717–5003    AALLTGATGFLGAFLLRDLLQMT
LtxA/2108–2397    SVLLTGATGFLGAYLLYELLKQT
MxcG/1094–1376    QVLLTGATGFVGAHLLDQLLRQT
NcpB/4438–4724    AILLTGATGFIGAFLLAELLQQT
SfmC/1102–1387    RVFLTGATGYLGLHLVEQLLRRT
Orf22/1078–1360   AVLLTGATGFLGSHLLDELQRAG
                       *  *  *
```

B)

```
PstD/569–885     YVSTADVGAAIEPSAFTEDADIRVISPTRTVDGGWAGGYGTSKW
PznA/2055–2290   YVSTISVGTYFD....IDTEDVTFSEADVYKGQLLTSPYTRSKF
KorD/616–895     YASTLSVLTG.........ERKWDEEDELVYSPDLMIGYSQSKW
LgrD/4717–5003   FVSTIFTFASEE....GEESVAVREEDMPENSRILTSGYTQSKW
LtxA/2108–2397   FVSTAAVAVSS.....KGNPDIIYENFRLGADSVLPSGYVSSKW
MxcG/1094–1376   YVSTLAVAPQA.....NLSPEVP EAFVP AHPGLRDGYQQSKW
NcpB/4438–4724   FISTVSVFASDE....YFKLDVVQENDPLEHSQGLLGGYTQSKW
SfmC/1102–1387   HVSTIDTLLAT.....HMPRPFLENDAPLHSAVGVPAGYTGSKW
Orf22/1078–1360  LISTLGVFPP......DSAPGVIGEDTVPGDPASLGIGYSQSKW
                    *                                  *   *
```

Figure S3. ClustalW alignment of reductase domains. Alignments were performed with MacVector 12.0.5 (MacVector Inc.) using the default parameters. **A)** NADPH binding region with identical residues shaded and the binding fingerprint residues marked (*) **B)** Catalytic triad region annotated as in (A).

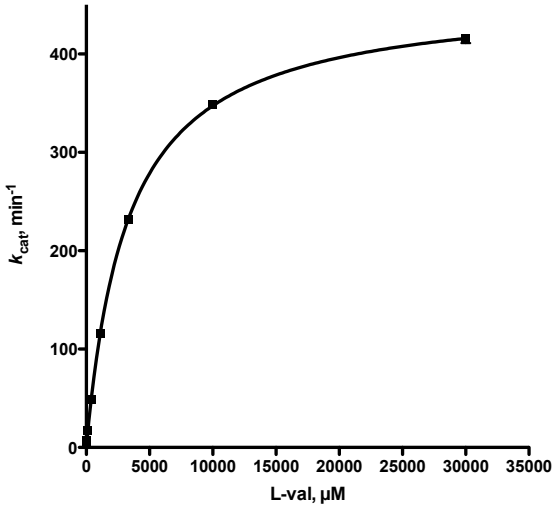

Figure S4. Exchange Assay steady state kinetics of AusA with Val. Each reaction contained 18 nM apo AusA, 375 mM Bicine pH 8.0, 10 mM $MgCl_2$, 3 mM ATP, 2 mM DTT, 1 mM pyrophosphate, 0.25 µci P^{32}pyrophosphate, and 41.2 µM — 30 mM Val. Velocities were fit to the Michaelis-Menten equation.

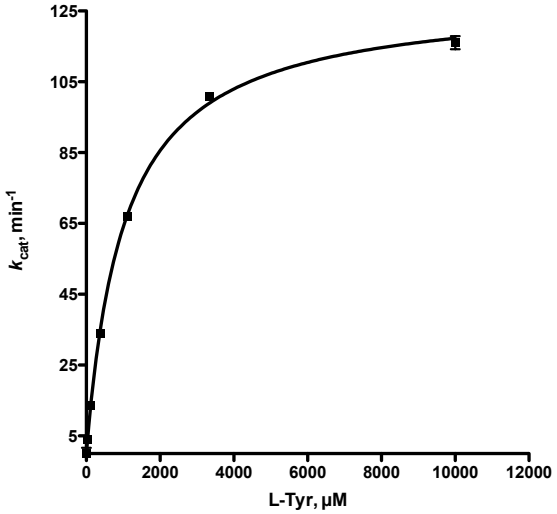

Figure S5. Exchange Assay steady state kinetics of AusA with Tyr. Each reaction contained 36 nM apo AusA, 375 mM Bicine pH 8.0, 10 mM $MgCl_2$, 3 mM ATP, 2 mM DTT, 1 mM pyrophosphate, 0.25 µci P^{32}pyrophosphate, and 41.2 µM — 10 mM Tyr. Velocities were fit to the Michaelis-Menten equation.

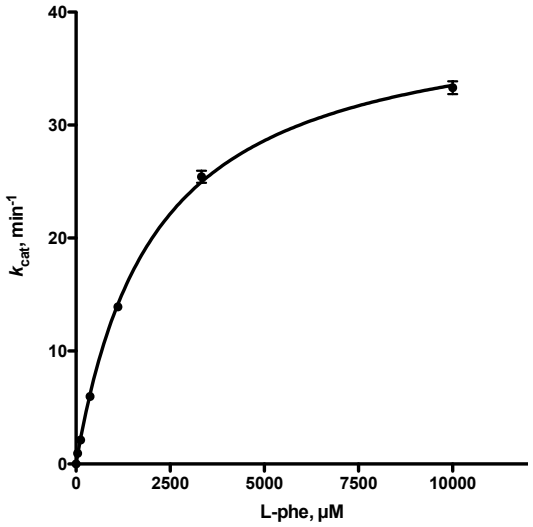

Figure S6. Exchange Assay steady state kinetics of AusA with Phe. Each reaction contained 72 nM apo AusA, 375 mM Bicine pH 8.0, 10 mM $MgCl_2$, 3 mM ATP, 2 mM DTT, 1 mM pyrophosphate, 0.25 µci P^{32}pyrophosphate, and 41.2 µM — 10 mM Phe. Velocities were fit to the Michaelis-Menten equation.

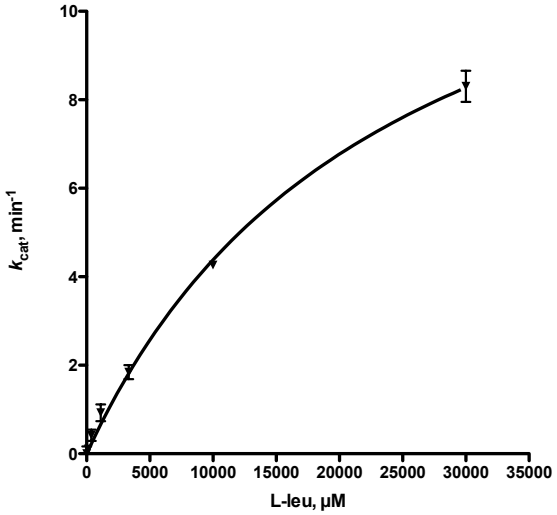

Figure S7. Exchange Assay steady state kinetics of AusA with Leu. Each reaction contained 72 nM apo AusA, 375 mM Bicine pH 8.0, 10 mM $MgCl_2$, 3 mM ATP, 2 mM DTT, 1 mM pyrophosphate, 0.25 µci P^{32}pyrophosphate, and 123.4 µM — 30 mM Leu. Velocities were fit to the Michaelis-Menten equation.

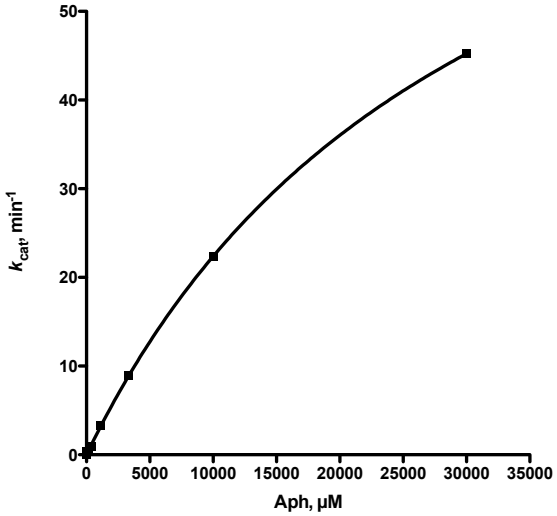

Figure S8. Exchange Assay steady state kinetics of AusA with Aph. Each reaction contained 72 nM apo AusA, 375 mM Bicine pH 8.0, 10 mM $MgCl_2$, 3 mM ATP, 2 mM DTT, 1 mM pyrophosphate, 0.25 μci P^{32}pyrophosphate, and 41.2 μM — 30 mM Aph. Velocities were fit to the Michaelis-Menten equation.

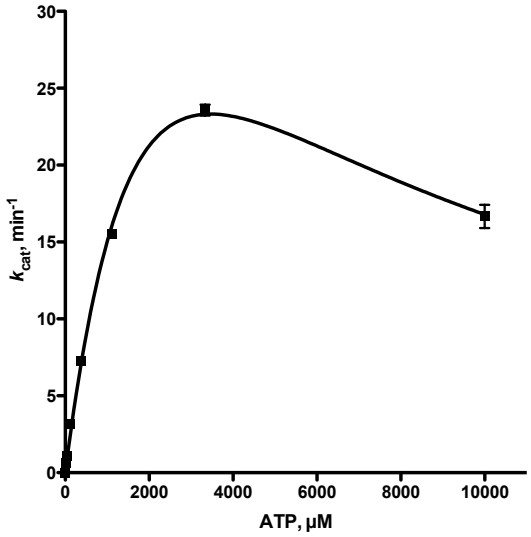

Figure S9. Exchange Assay steady state kinetics of AusA with ATP. Each reaction contained 36 nM apo AusA, 375 mM Bicine pH 8.0, 10 mM $MgCl_2$, 13.7μM — 10 mM ATP, 2 mM DTT, 1 mM pyrophosphate, 0.25 μci P^{32}pyrophosphate, and 30 mM Phe. Velocities were fit to the substrate inhibition equation.

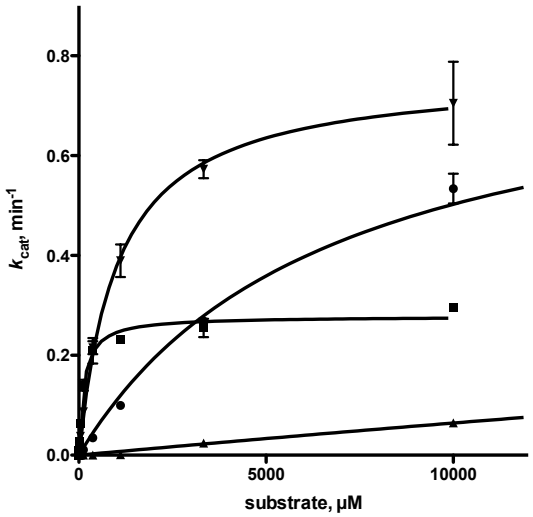

Figure S10. Product formation assay steady state kinetics of AusA for amino acids. Each reaction contained 40 nM holo AusA, 375 mM Bicine pH 8.0, 10 mM $MgCl_2$, 3 mM ATP, 0.1 mM NADPH, 1 mM TCEP, 5 mM Val and 13.7 µM — 30 mM Aph (●) or Leu (▲) or 4.6 µM — 10 mM Phe (▼) or Tyr (■) . Velocities were fit to the Michaelis-Menten equation.

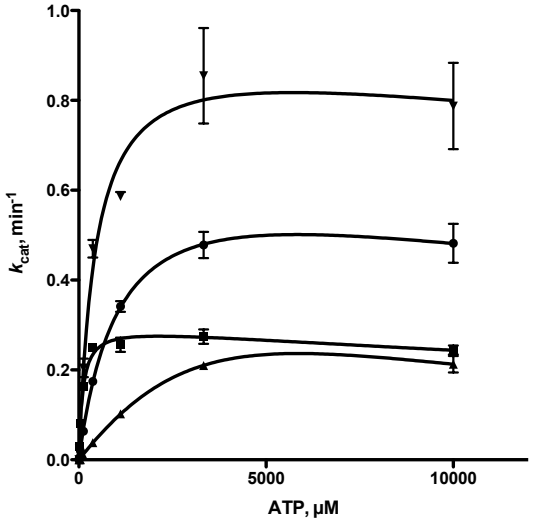

Figure S11. Product formation assay steady state kinetics of ATP. Each reaction contained 40 nM holo AusA, 375 mM Bicine pH 8.0, 10 mM $MgCl_2$, 13.7 — 10 mM ATP, 0.1 mM NADPH, 1 mM TCEP, 5 mM Val and either 10 mM Aph (●), Phe (▼), Tyr (■) or 30 mM Leu (▲). Velocities were fit to the substrate inhibition equation.

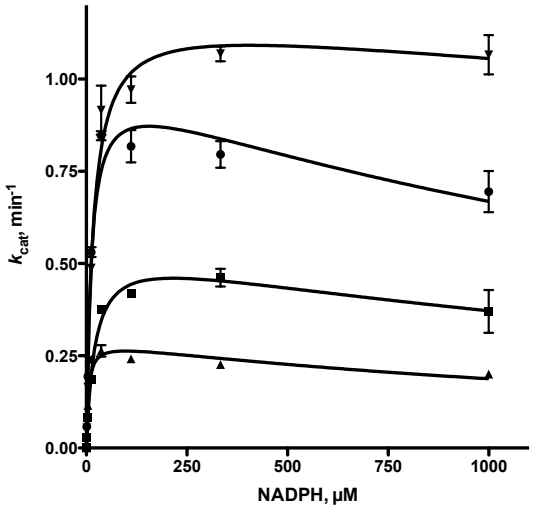

Figure S12. Product formation assay steady state kinetics of NADPH. Each reaction contained 40 nM holo AusA, 375 mM Bicine pH 8.0, 10 mM $MgCl_2$, 3 mM ATP, 1.4 μM — 1 mM NADPH, 1 mM TCEP, 5 mM Val and either 10 mM Phe (▼), Tyr (■), or 30 mM Leu (▲) Aph (●). Velocities were fit to the substrate inhibition equation.

References

(1) Qiao, C.; Gupte, A.; Boshoff, H. I.; Wilson, D. J.; Bennett, E. M.; Somu, R. V.; Barry, C. E. III; Aldrich, C. C.; 5'-*O*-[(*N*-Acyl)sulfamoyl]adenosines as antitubercular agents that inhibit MbtA: an adenylation enzyme required for siderophore biosynthesis of the mycobactins. *J. Med. Chem*. **2007**, *50,* 6080–6094.

(2) Declerck, V.; Nun, P.; Martinez, J.; Lamaty, F.; Solvent-free synthesis of peptides. *Angew. Chem. Int. Ed.* **2009**, *48*, 9318–9321.

(3) Zaramella, S.; Stromberg, R.; Yeheskiely, E.; Application of *N*-2,6-dimethoxybenzoyl histidine in solid-phase peptide synthesis; *Eur. J. Org. Chem.* **2003**, *2003,* 2454–2461.

(4) Abiko, T.; Onodera, I.; Sekino, H.; Synthesis of six analogs and their two fragments related to 1-α-hydroxyisovaleryl-Leu-Val-Phe-OMe as rennin inhibitor. *Biochem. Biophys. Res. Commun.* **1981**, *100*, 177–183.

(5) Ohta, A.; Akita, Y.; Takizawa, K.; Kurihara, M.; Masano, S.; Watanabe, T.; Synthesis of deoxymutaaspergillic acid and 2-hydroxy-3-isobutyl-6-isopropyl pyrazine 1-oxide. *Chem. Pharm. Bull.* **1978**, *26*, 2046–2053.

(6) Zeng, Y.; Li, Q.; Hanzlik, R. P.; Aube, J.; Synthesis of a small library of diketopiperazines as potential inhibitors of calpain. *Bioorg. Med. Chem. Lett.* **2005**, *15*, 3034–3038.

(7) Wyatt, M. A.; Wang, W.; Roux, C. M.; Beasley, F. C.; Heinrichs, D. E.; Dunman, P. M.; Magarvey, N. A.; *Staphylococcus aureus* nonribosomal peptide secondary metabolites regulate virulence. *Science* **2010**, *329*, 294–296.

(8) Vondenhoff, G. H. M.; Dubiley, S.; Severinov, K.; Lescrinier, E.; Rozenski, J.; Aerschot, A. V.; Extended targeting potential and improved synthesis of microcin C Analogs as antibacterials. *Bioorg. Med. Chem.* **2011**, *19*, 5462–5467.

(9) Conti, E.; Stachelhaus, T.; Marahiel, M. A.; Brick, P. Structural basis for the activation of phenylalanine in the non-ribosomal biosynthesis of gramicidin S. *EMBO J* **1997**, *16*, 4174–4183.

(10) Stachelhaus, T.; Mootz, H. D.; Marahiel, M. A. The specificity-conferring code of adenylation domains in nonribosomal peptide synthetases. *Chem Biol* **1999**, *6*, 493–505.

(11) Mitchell, C. A.; Shi, C.; Aldrich, C. C.; Gulick, A. M. Structure of PA1221, a nonribosomal peptide synthetase containing adenylation and peptidyl carrier protein domains. *Biochemistry* **2012**, *51*, 3252–3263.

(12) Kelley, L. A.; Sternberg, M. Protein structure prediction on the Web: a case study using the Phyre server. *Nat Protoc*. **2009**, *4*, 363–371.

(13) Arnaud, O.; Koubeissi, A.; Ettouati, L.; Terreux, R.; Alame, G.; Grenot, C.; Dumontet, C.; Pietro, A.D.; Paris, J.; Falson, P. *J. Med. Chem.* **2010**, *53*, 6720–6729.

(14) Deng, Y. et al. U.S. Patent 8,045,568, 2008.

(15) Bosch, M. P. Campos, F.; Niubo, I.; Rosell, G.; Diaz, J. L.; Brea, J.; Loza, M. I.; Guerrero, A.; *J. Med. Chem.* **2004**, *47*, 4041–4053.